Supporting Information for

Rolled-Up Optical Microcavities with Subwavelength Wall Thicknesses for Enhanced Liquid Sensing Applications

Gaoshan Huang,[†,*] *Vladimir A. Bolaños Quiñones,*[†] *Fei Ding,*[†] *Suwit Kiravittaya,*[†] *Yongfeng Mei,*[†,‡,*] *and Oliver G. Schmidt*[†]

[†]Institute for Integrative Nanosciences, IFW Dresden, Helmholtzstr. 20, D-01069 Dresden, Germany, and [‡]Department of Materials Science, Fudan University, Shanghai, 200433, People's Republic of China.

Address correspondence to gaoshan.huang@gmail.com, y.mei@ifw-dresden.de.

The resonant modes inside the optical microcavities are modelled analytically by the use of Maxwell equations. We consider the electromagnetic field propagating with an angular frequency ω, where time dependence of the harmonic wave is assumed as $e^{-i\omega t}$. It should be pointed out that no magnetic or metallic materials is employed, therefore $\vec{B} \equiv \vec{H}$ and the free current density is neglected ($\vec{J}=0$) in the Maxwell curl-field equations; with this, those equations are expressed as

$$\vec{\nabla} \times \vec{E} = ik\vec{B} \quad (1)$$

$$\vec{\nabla} \times \vec{B} = -ikn^2\vec{E} \quad (2)$$

where n is the material refractive index and $k=\omega/c=2\pi/\lambda_0$, being λ_0 the wavelength of the electromagnetic field and c refers to the air speed of light. In order to solve the Maxwell equations for our microtubular system we found a good approximation to treat the rolled spiral shape of the microtube as a planar waveguide with two regions (see the regions I and II in Figure S1) corresponding to the thicker and thinner part of the microcavity wall. Due to the symmetry of our structure in the *z* dimension (the axis of the tube), it is enough to solve the two-dimensional problem instead of the three-dimensional case. Thus the *z* component of the $\vec{\nabla}$ operator is taken as $\partial/\partial z=0$ in eqs. (1) and (2).

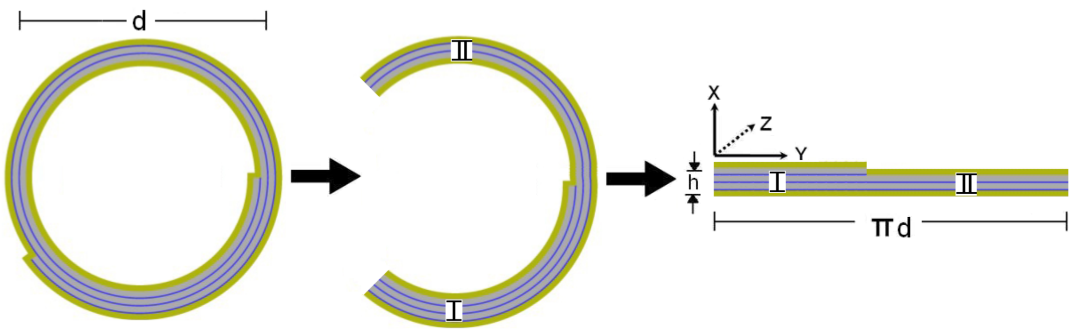

Figure S1. Cross sectional view of the structural changes of the spiral rolled-up microtube to a planar waveguide of two regions with different thicknesses.

The physical mechanism of the resonance modes comes from an electromagnetic wave propagating inside the microcavity wall and interfering constructively with itself after a round trip.[1] This condition must be adapted to the planar waveguide taking the wave propagating along the *y* dimension. Then, the *y* dependence of the electromagnetic fields is written by the function $e^{i\beta y}$, where β is the propagation constant. After a round trip ($y=\pi d$) the modes should have the same phase in order to get the constructive interference, thus $e^{i\beta y_0}=e^{i\beta\pi d}$. Choosing $y_0=0$ it is obtained that β should satisfy the resonance condition: $\beta=2m/d$, where *d* is the tube diameter and *m* is an integer (azimuthal number).

With the previous considerations, the spatial and temporal dependence of the electromagnetic field are in the form $\vec{A}(\vec{r})\equiv\vec{A}(x)\,e^{i\beta y-i\omega t}$ where $\vec{A}\equiv\vec{E}$ or $\vec{B}$. Therefore the components of the eq. (1) are given by

$$i\beta \mathrm{E}_z = ik\mathrm{B}_x \tag{3}$$

$$\frac{\partial \mathrm{E}_z}{\partial x} = -ik\mathrm{B}_y \tag{4}$$

$$\frac{\partial \mathrm{E}_y}{\partial x} - i\beta \mathrm{E}_x = ik\mathrm{B}_z \tag{5}$$

In the same way the components of the Maxwell eq. (2) have are given by

$$i\beta \mathrm{B}_z = -in^2 k\mathrm{E}_x \tag{6}$$

$$\frac{\partial \mathrm{B}_z}{\partial x} = in^2 k\mathrm{E}_y \tag{7}$$

$$\frac{\partial \mathrm{B}_y}{\partial x} - i\beta \mathrm{B}_x = -in^2 k\mathrm{E}_z \tag{8}$$

After eliminating the magnetic field $\vec{\mathrm{B}}$ or the electric field $\vec{\mathrm{E}}$ components from the last two set of equations, the wave equation for the *z* component is obtained,

$$\left[\frac{\partial^2}{\partial x^2} + (n^2 k^2 - \beta^2)\right] A_z = 0 \tag{9}$$

where $A_z \equiv \mathrm{E}_z$ or B_z. The modes can be classified as TM and TE polarization.[1] For the TM polarization the *z* component of the magnetic field is taken as $\mathrm{B}_z=0$, while for the TE polarization the *z* component of the electric field is taken as $\mathrm{E}_z=0$.[2] Here, detailed analytic derivation of the TM mode is carried out, for the TE case only the final expression is given due to a similar procedure.

TM resonant modes. In general, the electromagnetic field must decay exponentially outside of the wall and oscillates inside of it; hence the E_z component solution for the wave eq. (9) is,

$$\mathrm{E}_z = \cos\phi\, e^{-\delta x} \qquad \text{for} \quad x \geq 0 \tag{10}$$

$$= \cos(\gamma x + \phi) \qquad \text{for } 0 \geq x \geq -h \tag{11}$$

$$= \cos(-\gamma h + \phi)\, e^{\delta(x+h)} \qquad \text{for } x \leq -h \tag{12}$$

being ϕ a phase factor to be determined later and $\delta^2 = \beta^2 - n_2^2 k^2$, $\gamma^2 = n_1^2 k^2 - \beta^2$, where n_2 is the refractive index of the media surrounding the planar waveguide and n_1 is the average refractive index of the materials composing the planar waveguide. The E_z component is continuous at the interfaces where we assume h as the average waveguide height between the region I and II [see Figure S1] which is calculated by

$$h = a\, h_I + b\, h_{II}, \tag{13}$$

where a (b) is the length proportion of region I (region II) in the waveguide and h_I (h_{II}) the waveguide height at the region I (region II). From eq. (3) the B_x component is also continuous at the interfaces but the B_y component must be revised to satisfy this condition. Using the E_z solution and eq. (4), B_y is given by

$$B_y = -\frac{i}{k}\delta \cos\phi\, e^{-\delta x} \qquad \text{for} \quad x \geq 0 \tag{14}$$

$$= -\frac{i}{k}\gamma \sin(\gamma x + \phi) \qquad \text{for } 0 \geq x \geq -h \tag{15}$$

$$= \frac{i}{k}\delta \cos(-\gamma h + \phi) e^{\delta(x+h)} \qquad \text{for } x \leq -h \tag{16}$$

The B_y component does not immediately satisfy the boundary conditions. The requirement of continuity at $x=0$ and $x=-h$ leads to the following system of equations,

$$\gamma \sin\phi - \delta \cos\phi = 0 \tag{17}$$

$$[\delta \sin(\gamma h) + \gamma \cos(\gamma h)]\sin\phi + [\delta \cos(\gamma h) - \gamma \sin(\gamma h)]\cos\phi = 0. \tag{18}$$

Combining the last two equations results in the condition

$$\tan(\gamma h) = \frac{2\delta / \gamma}{1 - (\delta / \gamma)^2} \tag{19}$$

This transcendent function is solved finding the zeros numerically.

TE resonant modes. Employing a similar procedure used to the TM case but in this case taking $E_z=0$, the following expression is obtained

$$\tan(\gamma h) = \left(\frac{n_1}{n_2}\right)^2 \frac{2\delta/\gamma}{1-(n_1/n_2)^4(\delta/\gamma)^2} \tag{20}$$

Solution for the TM modes. The input parameters used for eq. (19) are the microcavity diameter, wall thickness, surrounding media refractive index n_2, and average refractive index of the waveguide n_1. First, it is necessary to calculate n_1 for our case where we have a bilayer nanomembrane of two different materials (n_{SiO2}=1.45 and n_{SiO}=1.55) which is coated on both sides with another material (n_{HfO2}=1.95) and with two regions of different heights. The method in literature [3] was employed to calculate the average dielectric constant ε ($\varepsilon = n^2$) of a bilayer system. The calculated average refractive indices (n_I and n_{II}) are different for the two regions (I and II, see Figure S1), therefore the final average refractive index n_1 is obtained by

$$n_1 = a\, n_I + b\, n_{II} \tag{21}$$

where a (b) is the length proportion of region I (region II) in the waveguide and n_I (n_{II}) the waveguide height at the region I (region II).

Table S1. Input parameters to calculate the resonant mode position

Diameter *d* [µm]	SiO thickness (nm)	SiO_2 thickness (nm)	HfO_2 thickness (nm)	Rotations in tube wall	Refractive index (water)	Refractive index (ethanol)
9	8	32	30	1.7	1.33	1.36

The resonant mode position is finally calculated as a function of the mode number m and the change of the refractive index which surrounds the optical microcavity, where the input parameters are listed in Table S1. In Table S2 the calculated mode positions are listed for the optical microcavity in three different surrounding media, within the wavelength range of 540 nm to 710 nm. For comparison, the mode positions from the experimental results and the finite-difference time-domain simulation (FDTD, which takes into account more details about the real structure of the optical microcavity) are also listed in Table S2, and a satisfactory agreement can be found, which supports the approximations performed in our analytical model.

Table S2. Mode positions, in wavelength (nm), from experimental results, FDTD simulation, and analytical calculation.

Dried	Experimental	544.50	551.27	558.09	565.44	573.04	580.64	588.24	596.63	605.01	613.65	622.56	631.72
Tube	FDTD	545.45	552.06	559.43	566.18	572.80	581.68	588.77	597.04	604.74	613.95	623.43	631.83
n_2=1.0	Analytical	542.34	549.24	556.33	563.63	571.14	578.86	586.82	595.03	603.48	612.21	621.22	630.53
Inside	Experimental	585.88	594.01	602.65	611.30	620.20	629.36	639.56	648.98	658.92	669.38	681.14	692.63
water	FDTD	586.66	595.02	603.50	611.95	620.64	630.57	639.36	649.30	659.25	670.15	680.92	691.86
n_2=1.33	Analytical	585.57	593.91	602.51	611.38	620.53	629.98	639.74	649.83	660.26	671.06	682.24	693.83
Inside	Experimental	594.53	602.65	611.82	620.72	629.62	639.83	649.25	660.49	671.99	682.18	693.94	705.17
Ethanol	FDTD	595.64	604.31	612.92	621.44	630.77	640.85	649.44	659.51	669.90	681.95	693.07	703.55
n_2=1.36	Analytical	593.09	601.66	610.50	619.62	629.02	638.74	648.78	659.16	669.89	681.01	692.52	704.44

References

1. Kipp, T.; Welsch, H;. Strelow, Ch.; Heyn, Ch.; Heitmann, D. Optical Modes in Semiconductor Microtube Ring Resonators. *Phys. Rev. Lett.* **2006**, *96*, 077403.

2. Bolaños Quiñones, V. A.; Huang, G. S.; Plumhof, J. D.; Kiravittaya, S.; Rastelli, A.; Mei, Y. F.; Schmidt, O. G. Optical Resonance Tuning and Polarization of Thin-Walled Tubular Microcavities. *Opt. Lett.* **2009**, *34*, 2345-2347.

3. Salandrino, A.; Engheta, N. Far-field Subdiffraction Optical Microscopy Using Metamaterial Crystals: Theory and Simulations. *Phys. Rev. B* **2006**, *74*, 075103.